MTL TR 92-5

AD

A SENSITIVITY ANALYSIS ON COMPONENT RELIABILITY FROM FATIGUE LIFE COMPUTATIONS

DONALD M. NEAL, WILLIAM T. MATTHEWS,
MARK G. VANGEL, and TREVOR RUDALEVIGE
MECHANICS AND STRUCTURES BRANCH

February 1992

Approved for public release; distribution unlimited.

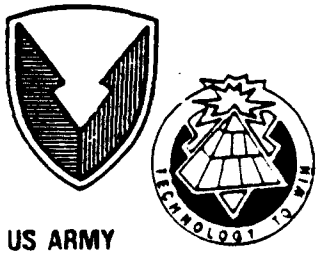

US ARMY
LABORATORY COMMAND
MATERIALS TECHNOLOGY LABORATORY

U.S. ARMY MATERIALS TECHNOLOGY LABORATORY
Watertown, Massachusetts 02172-0001

The findings in this report are not to be construed as an official Department of the Army position, unless so designated by other authorized documents.

Mention of any trade names or manufacturers in this report shall not be construed as advertising nor as an official indorsement or approval of such products or companies by the United States Government.

DISPOSITION INSTRUCTIONS

Destroy this report when it is no longer needed.
Do not return it to the originator

UNCLASSIFIED

SECURITY CLASSIFICATION OF THIS PAGE *(When Data Entered)*

REPORT DOCUMENTATION PAGE		READ INSTRUCTIONS BEFORE COMPLETING FORM
1. REPORT NUMBER MTL TR 92-5	2. GOVT ACCESSION NO.	3. RECIPIENT'S CATALOG NUMBER
4. TITLE *(and Subtitle)* A SENSITIVITY ANALYSIS ON COMPONENT RELIABILITY FROM FATIGUE LIFE COMPUTATIONS		5. TYPE OF REPORT & PERIOD COVERED Final Report 6. PERFORMING ORG. REPORT NUMBER
7. AUTHOR*(s)* Donald M. Neal, William T. Matthews, Mark G. Vangel, and Trevor Rudalevige		8. CONTRACT OR GRANT NUMBER*(s)*
9. PERFORMING ORGANIZATION NAME AND ADDRESS U.S. Army Materials Technology Laboratory Watertown, Massachusetts 02172-0001 SLCMT-MRS		10. PROGRAM ELEMENT, PROJECT, TASK AREA & WORK UNIT NUMBERS AMCMS Code: 612105.H8400
11. CONTROLLING OFFICE NAME AND ADDRESS U.S. Army Laboratory Command 2800 Powder Mill Road Adelphi, Maryland 20783-1145		12. REPORT DATE February 1992 13. NUMBER OF PAGES 23
14. MONITORING AGENCY NAME & ADDRESS *(if different from Controlling Office)*		15. SECURITY CLASS. *(of this report)* Unclassified 15a. DECLASSIFICATION/DOWNGRADING SCHEDULE

16. DISTRIBUTION STATEMENT *(of this Report)*

Approved for public release; distribution unlimited.

17. DISTRIBUTION STATEMENT *(of the abstract entered in Block 20, if different from Report)*

18. SUPPLEMENTARY NOTES

Presented at ARO sponsored Design of Exp. Conference at Vicksburg, MS, 22 October 1991.

19. KEY WORDS *(Continue on reverse side if necessary and identify by block number)*

Reliability	Probability density functions	Attack helicopters
Fatigue life	Monte Carlo method	
Flight loads	Probability	

20. ABSTRACT *(Continue on reverse side if necessary and identify by block number)*

(SEE REVERSE SIDE)

DD FORM 1 JAN 73 1473 EDITION OF 1 NOV 65 IS OBSOLETE

UNCLASSIFIED

SECURITY CLASSIFICATION OF THIS PAGE *(When Data Entered)*

Block No. 20

ABSTRACT

This paper identifies some uncertainties in determining high component reliability at a specified lifetime from a case study involving the fatigue life of a helicopter component. Reliabilities are computed from results of a simulation process involving an assumed variability (standard deviation) of the load and strength in determining fatigue life. The uncertainties in the high reliability computation are then examined by introducing small changes in the variability for the given load and strength values in the study.

Results showed that for a given component lifetime a small increase in variability of load or strength produced large differences in the component reliability estimates. Among the factors involved in computing fatigue lifetimes, the component reliability estimates were found to be most sensitive to variability in loading. Component fatigue life probability density functions were obtained from the simulation process for various levels of variability. The range of life estimates were very large for relatively small variability in load and strength.

CONTENTS

INTRODUCTION

Methodology to substantiate helicopter fatigue life has received considerable attention during the last decade. This interest was stimulated by the substantial variability in the results from the study on the American Helicopter Society pitch link problem.[1] Recently, further interest has resulted from the U.S. Army's introduction of a structural fatigue reliability criterion for rotorcraft. This criterion has been interpreted[2] as a requirement for a component lifetime estimate to have a reliability of 0.999999.

Helicopter safe life reliability methodology has recently been the subject of several papers[3-6] and an American Helicopter Society subcommittee round robin.[7]

The authors[8] have investigated the sensitivity of high reliability estimates from simple stress-strength statistical model computations. Results showed substantial variability in reliability estimates even for almost undetectable differences in the assumed probability density functions (PDFs) representing the stress and strength data.

In this report, the uncertainties in determining high reliability for helicopter component safe life design are studied by introducing a simulation process to identify the effects of a small amount of variability in the design variables for determining the lifetime estimate. The reliability values are determined for a generic uniaxial steel structure loaded in tension similar to a helicopter pitch link component by applying Miner's Linear Damage Rule.[9] The six component fatigue test values were obtained from Arden[1] where the maximum applied stress (S) on the component is tabulated with respect to cycles to failure (N). In order to obtain an SN curve to represent the component fatigue test results, a separate regression analysis was applied to a larger set of coupon tests of a steel for which the results are tabulated in Bury.[10] The assumed spectrum load used in determining the lifetime estimate was obtained from Berens.[11] Note that only the six component fatigue test values are from Reference 1 and the remaining test values are from References 10 and 11.

THE COUPON TEST SN CURVE

This section describes the procedure for determining an SN regression curve to represent coupon fatigue test data,[10] as shown in Figure 1. The assumed functional representation[12] of the data is

$$S = S_\infty + (S_u - S_\infty)e^{-\beta (\log_{10} N)^\gamma} \qquad (1)$$

where S is the maximum applied stress and N is the number of cycles required for the coupon to fail. S_∞ is the coupon endurance limit representing the case when $N \to \infty$ and S_u represents the static strength of the coupon; i.e., the strength for $N = 1$. The shape of the SN curve is determined by β and γ. S_∞, S_u, β, and γ were determined from application of an IMSL computer code[13] for solving nonlinear regression problems. The resultant SN curve is shown in Figure 1 (solid line) with the individual coupon fatigue test values.

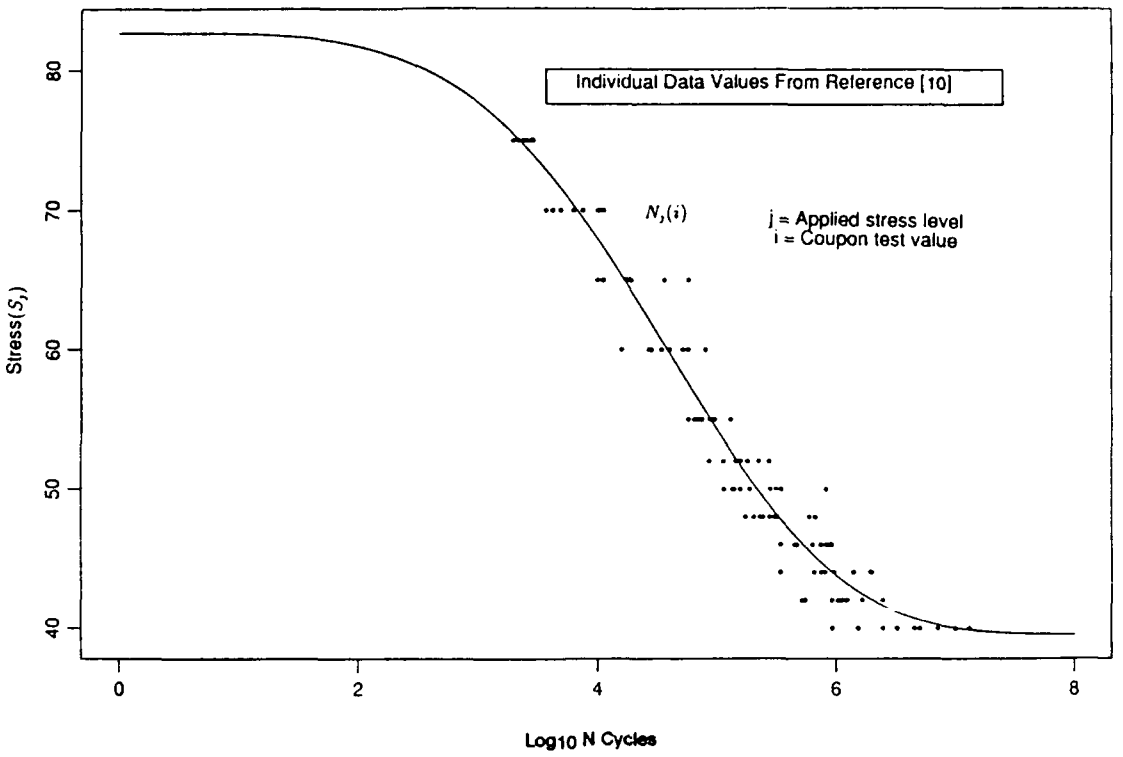

Figure 1. Mean coupon SN curve/fatigue data.

A review of the literature on the determination of component fatigue life showed that various functional representations similar to Equation 1 have been applied where N is the independent variable and S is the dependent (response) variable. This is counter to the conventional functional representation of test data where S would be the independent variable in the analysis since a *fixed* cyclic load (stress) value is applied and a *resultant* (dependent) number of cycles to failure is recorded. In order to obtain N as the dependent variable, Equation 1 can be inverted resulting in the following:

$$\log_{10} N = e^{\{\log[-\log((S - S_\infty)/(S_u - S_\infty))] - \log\beta\}/\gamma} \quad (2)$$

Although Equation 2 is recommended in determining the functional representation of the data, Equation 1 was applied in this study since it is commonly used in engineering fatigue analysis, and the qualitative measure of the relative uncertainties in determining the reliability at a specified lifetime are not affected by the SN curve assumption.

In order to simplify the analysis, the fatigue data from Reference 10 was normalized with respect to the estimated S_∞ value determined from the initial application of regression analysis. Another SN curve was then obtained from the normalized data, where β, γ, and S_u were obtained for a known S_∞ of 1. The resultant SN(N) curve is shown in Figure 2. The figure also shows the regression results SN(S) from the application of Equation 2.

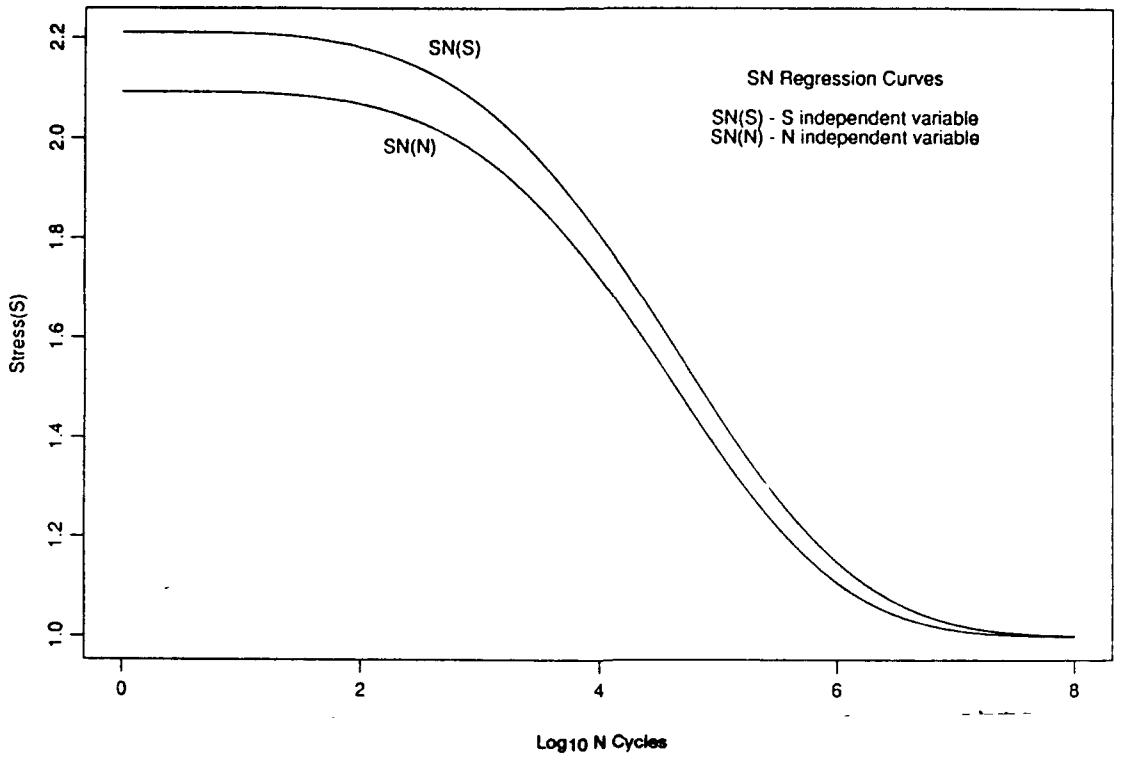

Figure 2. Regression curves from coupon test results.

THE COMPONENT SN CURVE

Usually the shape of the component SN curve is obtained from a prior coupon SN(N) curve, as shown in Figure 2. The location (ordinate position) of the curve is determined from extrapolating the individual component values, as shown in Figure 3, to N = 10^8 cycles. The original component values in Reference 1 have been rescaled so that they have scales similar to the S values in Figure 2. The extrapolation process involves vertically positioning the coupon SN curve (see Figure 3) to agree with the individual component values and then extending the curves to N = 10^8 cycles. S_i values are obtained for N = 10^8 and the component curves mean stress position at N is

$$S_m = \sum S_i / n, \tag{3}$$

where n is the number of component test results. The solid line in Figure 4 shows the representative component SN_c curve and component test data. Since there are usually only six component test results available, because of the costs in component testing, the above procedure is often applied. Using the more extensive, less expensive coupon test results to determine the shape of the SN curve assumes similar material, test, and environment for both coupon and component.

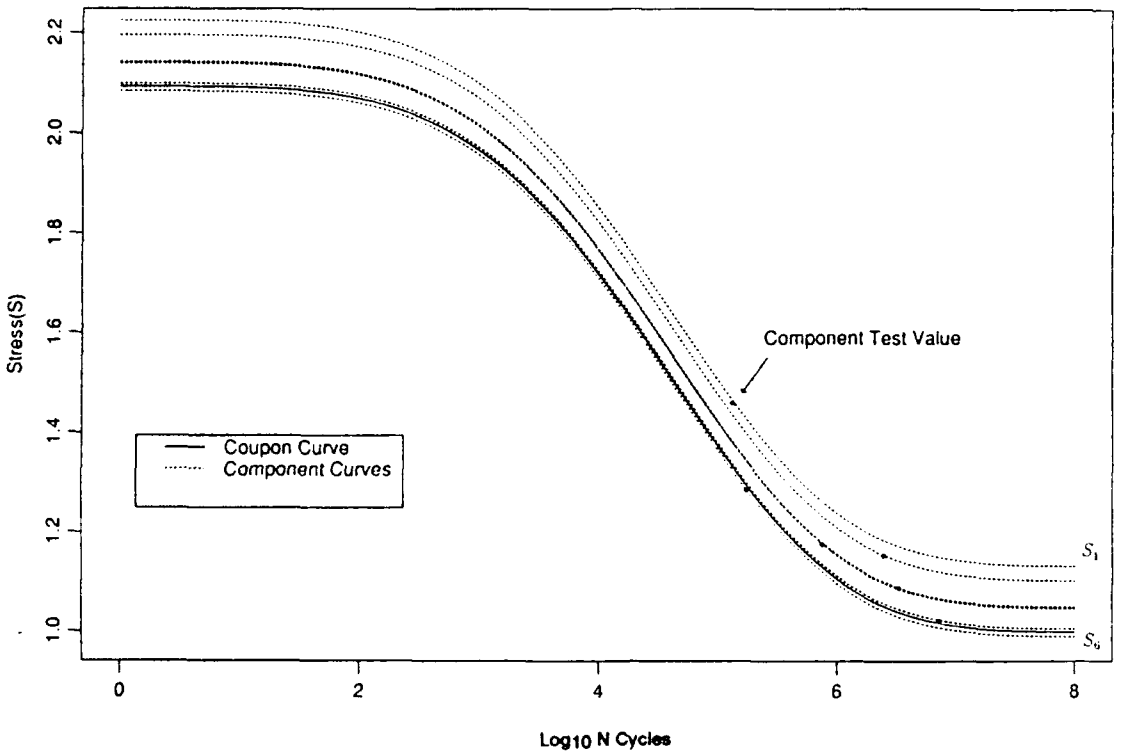

Figure 3. Extrapolation of component data.

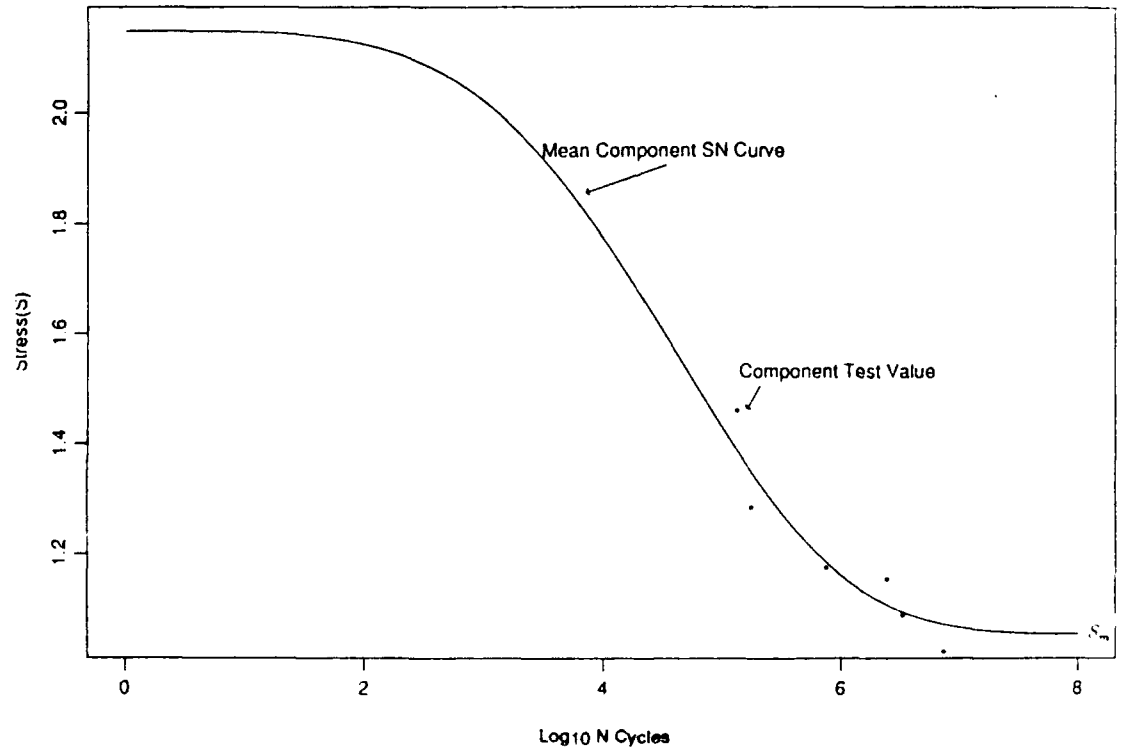

Figure 4. Mean SN curve for component test values.

SPECTRUM LOAD

The normalized spectrum loading used in the fatigue life analysis is shown in Figure 5a. The loading was obtained from a rainflow count of a modified combat history described in Reference 11. The spectrum was determined by the number of loads within discrete range increments. The spectrum is simplified to five loads $\{L_i\}_1^5$ by expanding the size of the range increments and including the appropriate cycle count $\{n_i\}_1^5$ within each expanded range. The normalization procedure involved dividing each L_i by the smallest damaging load S_∞ (endurance limit). This simplification was adequate for identifying the spectrum effects in this study.

MINER'S RULE

In order to obtain the lifetime estimate from the simplified fatigue load (L) and the normalized material strength (S) data shown in Figures 5a and 5b, the following linear damage rule[9] is applied where

$$DF = \sum_{i=1}^{5} \frac{n(i)}{N(i)} \tag{4}$$

is the damage fraction for each pass or repetition of the spectrum. This representation of operation hours is described in Reference 10. The n(i)s are the number of cycles corresponding to the applied load L(i), as shown in Figure 5a. The N(i) values are obtained from the SN curve, as shown in Figure 5b, where the corresponding S_i values are identified in the figure by the L(i) values obtained from the spectrum loads in Figure 5a. In addition, the rule requires that

$$N_P \cdot DF = 1 \tag{5}$$

in order to determine the maximum number of passes (N_P) that can occur prior to the component failure.

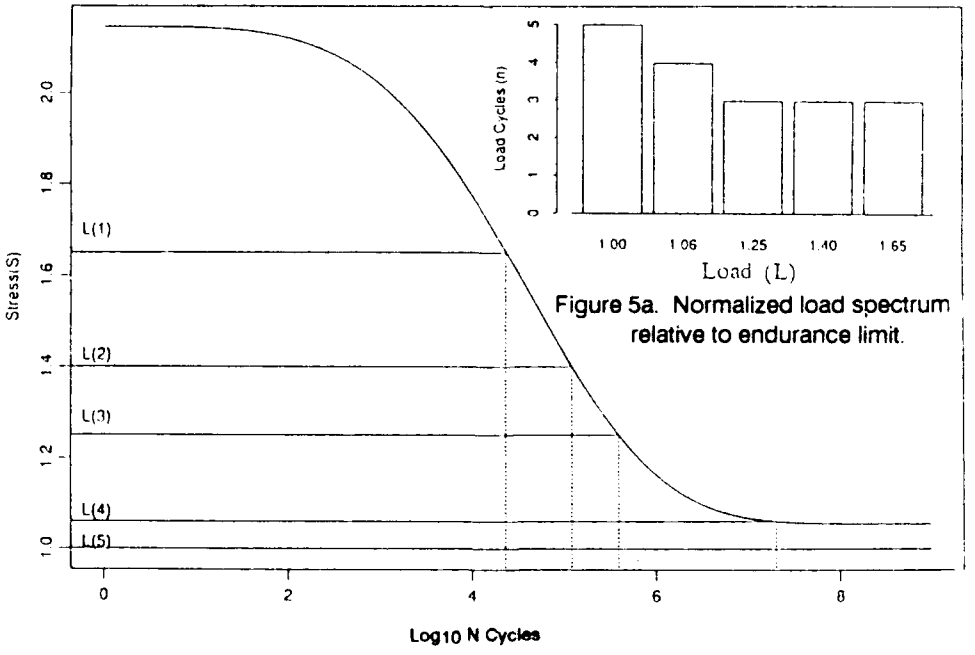

Figure 5a. Normalized load spectrum relative to endurance limit.

Figure 5b. Component mean SN curve.

SIMULATION PROCEDURES IN DETERMINING COMPONENT RELIABILITY

Bootstrap Method Applied to Coupon SN Curve Computation

The Bootstrap Method,[14] a simulation process, was introduced in the fatigue life reliability analysis in order to examine the effects of uncertainties used in determining the coupon SN curve and the resultant component reliability. Only one reliability estimate can be obtained from a single set of data; however, even with all conditions the same, one would expect to determine a different reliability estimate from another set of data. The Bootstrap Method provides a technique for estimating the variability among random sets of data generated under equivalent conditions using data from only a single random sample. The idea is to create arbitrarily many *new* datasets by sampling *with replacement* from the original data. If there are n values in the original data, then a new dataset is created by selecting n values from among these observed data, allowing data values to be selected more than once. The probability distribution of the reliability calculated from these datasets, which are created by taking random samples from the single observed dataset, provides an estimate of the actual probability distribution of reliability which could, in principle, be determined from *future* datasets.

The material fatigue testing involves obtaining the number of cycles to failure for a specified applied load (S) shown as the individual data points in Figure 1. The Bootstrap Method involves selecting a random set of 9 values independently with replacement from the set of cycles to failure values $\{N_j(i)\}_{i=1}^{9}$ for each j^{th} applied stress from $\{S_j\}_1^{12}$, as shown in Figure 1 and obtained from Reference 12. The result is a new set $\{N_j^*(i)\}_1^9$ for each of the S_j values. The new set is called the *Bootstrap* sample where some values can be repeated once, twice, or more times. The new set is then used in the regression procedures described in the Coupon Test SN Curve Section in order to obtain a new SN curve (S in Equation 1).

In Figure A1 (see Appendix), the results of applying the Bootstrap show a 90% confidence band on the original SN(N) curve. Results in Figure A2 show the individual SN(N) curves obtained for the Bootstrap samples. The results from Figures A1 and A2 indicate that there is more variability for large or small N values than for the central region of the curve which is consistent with determining confidence bands on regression curves.

For calculating the effects of coupon SN curve uncertainties, a damage fraction (DF*) value is computed by applying the linear damage rule. The above procedure is repeated M_B times, so that a set of $\{DF_k^*(i)\}_1^{M_B}$ are obtained. The component reliability R can then be obtained by counting the number (N_B) times $N_P \cdot DF^* < 1$, $k = 1,2,...,M_B$, where N_P, the number of passes, is specified. The computed component reliability R including uncertainties in the coupon testing procedure is written as

$$R = N_B / M_B, \tag{6}$$

where M_B is the number of repeated applications of the Bootstrap procedure.

Reliability Estimates from SN Component Curve Simulations

The following simulation procedure was applied in order to identify the effects of uncertainties in the location of the component SN_c curves on the reliability estimates.

*Represents simulation results.

The uncertainties are assumed because of the potential differences in loading, material, surface conditions, and geometry between the coupon and component. Also contributing to these uncertainties are: the extrapolation of the component fatigue data in determining the S_i's, as shown in Figure 3, and the availability of only six values in computing S_m (mean of the curve), as shown in Figure 4. Examination of potential inaccuracies in the reliability computations due to assuming that the component and coupon SN curve shapes are similar was not included in the simulation process. Introducing variability in the curve's location was sufficient for showing sensitivity in the reliability computation. In the simulation process, a random set of M S^*_m values were obtained. These values are normally distributed about the S_m value in Figure 4 from the following:

$$S^*_m(i) = S_m(1 + V_S \cdot Z_i),\ i = 1,2,...,M\,, \tag{7}$$

where the Z_i's are values randomly selected from a standard normal distribution with a mean of 0 and a variance of 1. The V_S value is the coefficient of variation (CV) and the mean is S_m. In Figure A3, a representative normally distributed set of S^*_m values are shown for V_S = 0.01 and V_S = 0.02. The newly obtained mean values (S^*_m) are now used in vertical positioning of the component SN curve, as shown in Figure 4, so that M SN curves can be obtained from Equation 1 by the following:

$$S^*_i = S\,(S_\infty, S_u, \beta, \gamma) + \Delta P_i\,,\ i = 1, 2, ..., M\ , \tag{8}$$

where $\Delta P_i = S^*_m(i) - S_m$. M damage fraction values (DF^*_i) are obtained from applying the procedures described in the Miner's Rule Section and the schematics shown in Figures 5a and 5b using the newly available S^*_i values.

From Miner's Rule, compute $N_P \cdot DF^*_i$, i = 1, 2, ..., M and record the number (N_S) of times $N_P \cdot DF^*_i < 1$ for a given N_P value, where N_P represents the specified number of passes. The component reliability R can be written as

$$R = N_S / M\,. \tag{9}$$

Note that in order to obtain 0.999999 reliability, M = 1 x 10^6 simulations would be required.

Load Uncertainties Effect On Reliability Computations

A simulation procedure similar to that described in the previous section was applied in order to identify the sensitivity in computing component reliability by introducing uncertainties in the assumed spectrum loads (see Figure 5a). There exist potential errors involved in assuming a specific load spectrum.[15] They are the results of: an inaccurate measuring device, the location of the device, and assuming load patterns determined from short periods of data recording which differ from the actual loads the component would be subject to during its operational lifetime.

Application of the simulation process involved only modeling uncertainties in the L values, with n(i)s remaining constant for a given load. Introducing the same amount of variability in each $\{L(i)\}_1^5$ values was sufficient to show the sensitivity of the reliability estimates from uncertainties in the loading.

Initially, the simulation involves obtaining M1 sets where the j^{th} set $\{L_j^*(i)\}_{i=1}^{5}$ is determined from the following:

$$L_j^*(i) = L(i)(1 + V_L \cdot Z_j), i = 1,2,...,5 \quad (10)$$

where $j = 1,2,...,M1$ and Z_j is a random value from a standard normal N(0,1) distribution. V_L is the coefficient of variation representing an assumed variability in load L(i).

For the j^{th} simulation, the original five loads $\{L(i)\}_1^5$, as shown in Figure 5a, are modified resulting in a new set $\{L_j^*(i)\}_i^5$ from Equation 10. The distribution of $L_j^*(1)$ for all j values, for example, would be similar to that for S_m, as shown in Figure A3.

In the simulation process, the j^{th} modified set L_j^*, and its associated N_j^*, determines a damage fraction value DF_j^*, as described in the Miner's Rule Section and Figures 5a and 5b. In order to obtain component reliability values from the load variability, Miner's Rule is then applied by recording the number (N_L) of times $N_P \cdot DF_j^* < 1$ for $j = 1,2,...M1$. The component reliability R is then written as

$$R = N_L / M1 . \quad (11)$$

Reliability Sensitivity from Uncertainties in Miner's Rule

A simulation procedure similar to those in the previous two sections is applied to the Miner's Rule relationship in Equation 5. This was done in order to examine the effects of a possible error in assuming the component will fail when $N_P \cdot DF = 1$ (see Equation 5). In order to identify the effects of this uncertainty in computing component reliability R, the following simulation process was performed:

Initially, the value 1 in Equation 5 is replaced by a set of random numbers $\{CR_i\}_1^{M2}$ resulting in $N_P \cdot DF^* < CR_i$, where

$$CR_i = 1 + V_M \cdot Z_i , i = 1,2, ..., M2 \quad (12)$$

and V_M and Z_i are the assumed coefficient of variation and standard normal as previously defined in the above two sections.

The reliability R is determined from recording the number (N_Z) of times that

$$N_P \cdot DF^* < CR_i , \quad (13)$$

and then defining

$$R = N_Z / M2 \quad (14)$$

where M2 is the number of simulations.

WORKING SN CURVE

The adjustment of the mean component SN_c curve from a limited amount of component test data results in a certain amount of variability in estimating the location of the curve. In order to account for this variability, and in some instances other uncertainties in the fatigue analysis process, a component SN_c curve reduction factor is often introduced which results in a new working SN_w curve, as shown in Figure A4. There is no standard method for obtaining a working curve in the helicopter industry.[16] The working curve in Figure A4 was obtained by a uniform reduction in all S_c values. This approach maintains the same curve shape as in the original SN_c curve; i.e., the coupon SN curve shape. This approach is consistent with the use of the coupon curve shape in the extrapolation process for each component data value (see Figure 3) by which the original component curve S_m value (see Figure 4) is obtained. In Figure 3, a schematic of this uniformity is shown where for $N = 1$ and $N = 10^8$ show an equal amount of assumed dispersion in the S_i values.

Reduction Factors for Working Curves

Some of the reduction factors commonly used by the helicopter manufacturers are discussed in References 15 and 16. In some cases a multiplication factor is used to obtain working curve values, S_w; i.e.,

$$S_w = S_c - P \cdot S_m \tag{15}$$

where S_c represents the strength values from the component curve, SN_c for various P values. S_m was previously defined in Equation 3.

Another reduction procedure involves defining

$$S_w = S_c - 3 \cdot SD \tag{16}$$

where the standard deviation (SD) is often determined from an assumed standard coefficient of variation for a particular material to represent the S_i values shown in Figure 3 and in Equation 3. A typical value for the coefficient of variation for steel is 7%. The SD value is then written as $SD = 0.07 \cdot S_m$. One other method involves determining SD from the actual S_i values; i.e., $SD = \sqrt{(\sum (S_i - S_m)^2 / (n-1)}$, and substituting the SD value in Equation 16.

The working curve was introduced in this report in order to evaluate its capability to include the possible variability in the reliability estimates from the simulation results.

RESULTS AND DISCUSSIONS

In this section, results from the simulation procedures are shown in both tabulated and graphical form. Variability is introduced in combination, as well as individually, for all of the following four factors: the spectrum load, the mean SN Curve, Miner's Rule, and the Bootstrap process.

In Table 1 all four factors were varied for a range of CV values (% variability) from 1% to 5%, except for the Bootstrap simulation where the variability is obtained from coupon test results. The component reliability results are tabulated as a function of the corresponding CV values assumed in the simulation procedures. The results were obtained by systematically randomly selecting values from each of the four factors so that 1×10^6 distinct factor combinations are obtained for computing the damage fraction (DF) in the Miner's Rule Section. The reliability (R) is then obtained from the sum of all the times $N_P \cdot DF^* < 1$ divided by 1×10^6.

Table 1. RELIABILITY VERSUS FACTOR VARIABILITY: LIFETIME = 3425

% Variability*	Reliability
1.0	0.999999
2.0	0.989676
3.0	0.937250
4.0	0.872101
5.0	0.816061

*Simultaneous variability assumed for the following: spectrum load, mean curve, Miner's Rule = factor (1) and the Bootstrap process on defining mean curve are applied.

In order to apply the simulation procedures, a 1% variability was introduced for each of the factors and the number of passes (N_P = 3425) was selected in order to obtain a baseline reliability value of 0.999999. This value was selected because of the helicopter industry's interest in obtaining high component reliability of 0.999999.

The results in Table 1 show a substantial instability when comparing the reliability estimate of 0.999999 versus 0.989676 for the respective 1% and 2% variabilities. The implication of these results is that in one case one in a million failures could occur compared to 10324 failures in a million in the other. This substantial difference for such a small increase in the inherent variability in the assumed fatigue life models shows a severe sensitivity in computing high reliability when there is a small degree of uncertainty in determining spectrum loads, SN curves, and assuming a failure requirement from Miner's Rule. The results from increasing the variability from 3% to 5% show a corresponding reduction in reliability values. The R = 0.816061 for 5% variability is a very large reduction from the original 0.999999 for 1% variability. The CV values shown in Table 1 represent a range of potential parameter uncertainties in the fatigue life model.

In Table 2, reliability values are tabulated as a function of the combined and individual variability of the four factors. This was done in order to examine the effects of the individual factor variability on computing component reliability. The 1% variability was applied to all factors resulting in R = 0.999999 when N_P is equal to 3425 (as in Table 1 at 1%). The 2% variability was applied to each factor individually with 1% variability for the other two factors. The Bootstrap process was applied in all of the cases. Introducing a 2% CV in the spectrum load (SPL) shows a substantial reduction in the reliability estimate from 0.999999 to 0.996404. The 2% variability in the component SN_c curve (MSN) shows a smaller reduction of 0.999999 to 0.999440 indicating that, based upon the particular spectrum considered, the *spectrum load uncertainties* could result in greater instability in the reliability values. Small variations in the Miner's Rule assumption (see Equation 13) do not appear to be as critical in the reliability computations. Increasing the variability from 3% to 5% shows a continued decrease in reliability estimates except for the case of Miner's Rule variability which has a very small reduction. The 5% variability on the spectrum load shows a value R = 0.862469 which is only 5.7% greater than the case where all factors were varied simultaneously, as shown in Table 1 for 5% variability.

Table 2. RELIABILITY VERSUS INDIVIDUAL FACTOR VARIABILITY: LIFETIME = 3425

% Variability (P) on Individual Factors*	Reliability		
	SPL	MSN	MR
1.0	0.999999	0.999999	0.999999
2.0	0.996404	0.999440	0.999998
3.0	0.967356	0.992375	--------
4.0	0.912587	0.972164	0.999997
5.0	0.862469	0.941979	0.999994

*1% variability is applied to all factors except for individual increase in factor variability (P) in first column. Bootstrap process also included.

In Table 3, reliabilities are obtained for the individual factors, spectrum load (SPL), and location component SN curve (MSN). In order to obtain the R = 0.999999 value for 1% variability on each of the factors, the number of passes (N_P) was 3700 for SPL and 4425 for MSN. The lower N_P value for SPL is consistent with the results in Table 2 since the R values for SPL were lower than those for MSN when N_P was 3425. In addition, it is obvious that a lower number of cycles of operation would usually increase the reliability value. The Bootstrap Method application resulted in a value of R = 0.999977 when combined with a 1% variability in MSN. This indicates that the method is not introducing any substantial variability compared to the SPL and MSN contribution in determining R. This is expected because of the small amount of variability in the SN curves, as shown in Figures A1 and A2. In addition, the range of cycle values contributing the most in determining the damage fraction has the least amount of variability.

Table 3. RELIABILITY VERSUS INDIVIDUAL FACTOR VARIABILITY / LIFETIME

% Variability	Reliability (R)	
	SPL*	MSN†
1.0	0.999999	0.999999
2.5	0.969376	0.965875
5.0	0.828010	0.818789

*3700 Lifetime value
†4425 Lifetime value
NOTE: Application of Bootstrap process simulation resulted in R = 0.999977 with 1% variability for MSN.

Table 4 shows the reliability results from reducing the S_m value, shown in Figure 4 and Equation 3, by the tabulated percentage in order to examine the possible material mean strength loss from environmental effects such as corrosion. New values equal $(1 - p/100)S_m$ where p is the tabulated percent reduction factor. In the case where p = 0, R = 0.999999 was obtained varying the SN_c curve by 1% with N_P = 4425 which is in agreement with the result in Table 3. This variability in the SN_c curve (MSN) was maintained for each of the reduced S_m values. When p = 1, then $0.99S_m$ was used in the simulation process to obtain a reliability value equal to 0.999852 compared to 0.999999 for no reduction in S_m. This result is not as substantial a reduction in R as the case where the S_n value is reduced by 5% and R = 0.324206. The overall results indicate that loads which previously did not increase the damage fraction are now significant contributors in reducing the component reliability. If there is a potential for material strength loss due to corrosion, for example, then high reliability estimates are substantially reduced by small mean strength reduction.

Table 4. RELIABILITY VERSUS PERCENT REDUCTION MSN: LIFETIME = 4425

% Reduction	Reliability
0.0	0.999999
1.0	0.999852
2.0	0.995542
3.0	0.946600
4.0	0.720650
5.0	0.324206

NOTE: 1% variability on MSN

Table 5A shows the deterministic fatigue lifetime values obtained from the application of various working curves described in the Working SN Curve Section. This computation was introduced to evaluate the curves relative effectiveness in accounting for the uncertainties in estimating the component SN_c curve. This evaluation involves comparing results from Tables 5A and 5B. In Table 5A, P = 0.5 which is the reduction from S_c in Equation 15. This shows a lifetime of 0.325, which is a very conservative estimate compared to the 6150 passes obtained from using the original component curve without a reduction. The least conservative lifetime estimate is 2000 which was obtained from reducing the component curves by three SDs. SD was obtained by using the S_i values in Figure 3 and Equation 3. This estimate was less conservative than the 1225 lifetime value obtained using an assumed CV = 0.07. The extrapolation process shown in Figure 3 may account for the relatively low SD estimate for the case when the life value is 2000. The other reduction factors result in a predictable decrease in the life estimate with an increase in the reduction percent P.

Table 5A. LIFETIME VALUES FROM APPLICATION OF WORKING CURVES

Working Curve (Adjustment on S)	Lifetime Value
0.50*	0.325
0.44	48
0.30	500
0.25	850
0.20	1355
S - 3(sd)†	1225
S - 3(sd)	2000
NA ◊	6150

*Percent reduction of (P) on S: where (1-P)S is location of working curve and S is mean component strength at endurance limit.
†Standard deviation determined from assuming 7% coefficient of variation for S.
◊ NA: No adjustment of SN curve.

Table 5B. LIFETIME VALUES WITH 0.999999 RELIABILITY VERSUS VARIABILITY ON MSN AND SPL

% Variability	Lifetime Value
1.0	3425
2.0	1850
3.0	875
4.0	350
5.0	50

In Table 5B, simultaneous variability on the component curve (MSN) and the spectrum load (SPL) for 0.999999 reliability shows a reduction in the lifetime value with increasing variability, which is consistent with prior results. By comparing results from Tables 5A and 5B the effectiveness of the working curve in obtaining 0.999999 reliability can be identified. That is, for example, a 1% variability shows 3425 indicating that any of the working curves could provide the required reliability although the curve obtained from the three SD reductions would be the least conservative acceptable method. Introducing 2% variability shows a life estimate of 1850 which, in this case, requires using the three SD reduction procedure where SD is obtained from assuming a 0.07 CV value. If the variability is assumed to be 5%, then a lifetime value of 50 is obtained which would require a working curve reduction factor of 0.44 in order to provide the 0.999999 reliability. If a 5% variability in the loading and SN curve can exist, then most of the working curve procedure would be an undesirable method for obtaining high reliability.

Using Equation 7, the results of introducing a 1% uncertainty in the positioning of the component curve is shown in Figure 6 as a probability density function for the lifetime estimate ($N_P = 1/DF$) determined from Equation 4. A 7.3% coefficient of variation was obtained with a mean life of 6194. The inner range, $N_P \pm 3 \cdot SD$, is 4964 to 7689 when the function is assumed to be log-normal; this is a substantial variability in the life estimate for a very small amount of variability in the location of the SN curve.

In Figure 7, a density function for the life estimate was obtained from an assumed 5% variability using the same procedures as described above. In this case, the CV was 37.5% with a mean equal to 6621. The inner three SD range is 2065 to 18587 for the lifetime value estimates. This exceptionally large dispersion in the life estimates for a moderate amount of variability (5%) in the location of the mean curve indicates instability in estimating lifetime values. It is noted that by taking the log of the data, a normal function was obtained indicating that the fatigue estimate can be represented by a log-normal distribution.

In Figure 8, a computation similar to that described in Figure 6 was performed in order to determine the difference in life values between 1% and 0.0001% points corresponding to reliabilities of 0.99 and 0.999999, respectively. A 1% variability in the spectrum was assumed in the computation of N_P. A CV of 10.8% was obtained with a mean of 6203. Results show a life of 4795 for the lower reliability of 0.99 and 3689 for the higher reliability of 0.999999 showing a 23% decrease in the lifetime estimate.

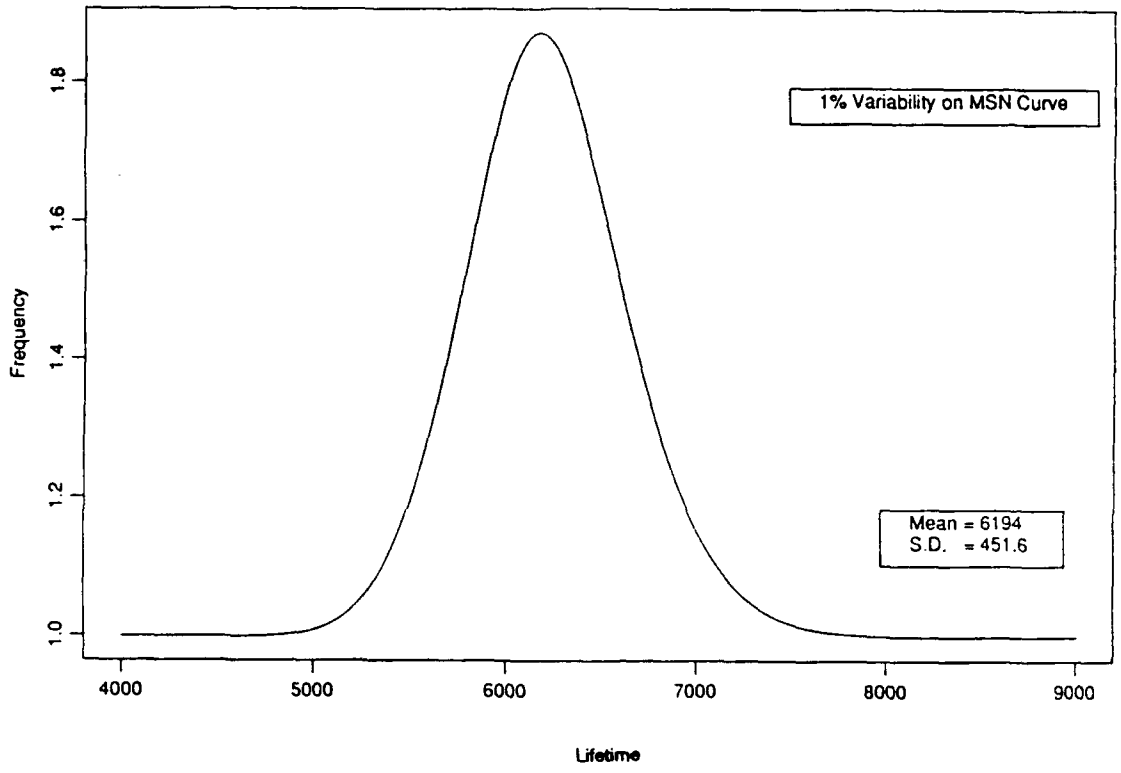

Figure 6. Component fatigue life probability density function.

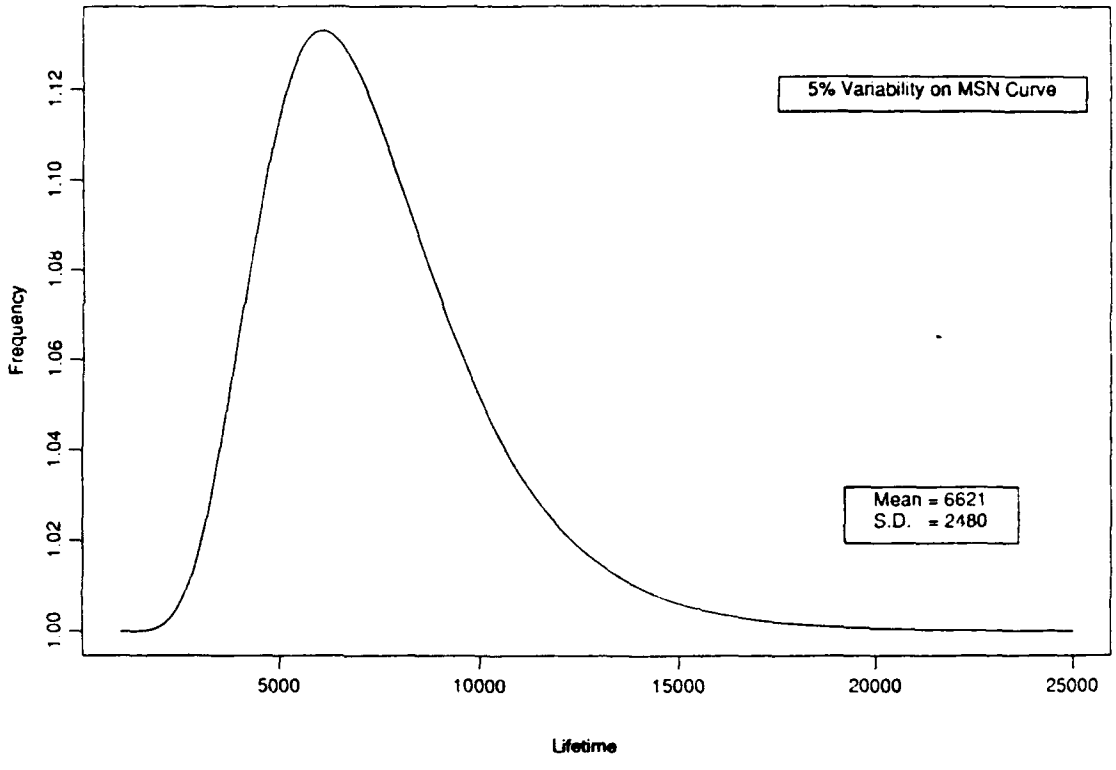

Figure 7. Component fatigue life prability density function.

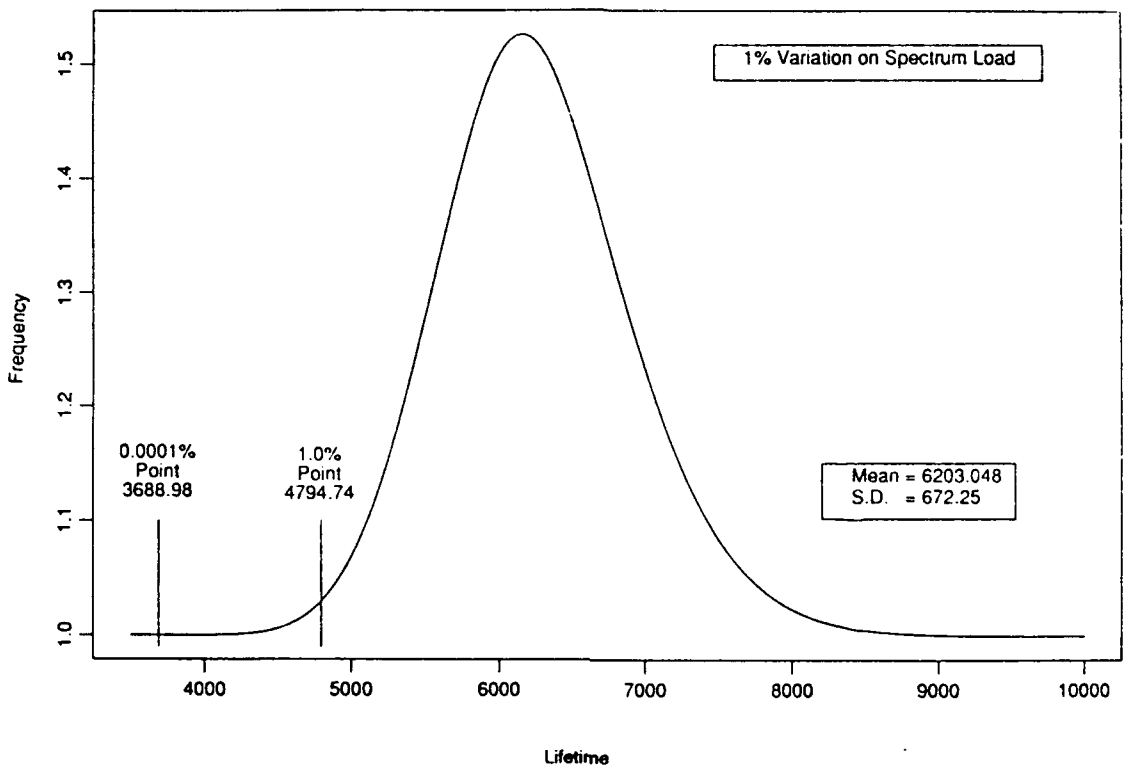

Figure 8. Component fatigue life probability density function and reliabilty.

Figure 9, where a 5% variability in the spectrum load was introduced, shows a log-normal distribution of lifetime values similar to that in Figure 7 for the SN_c curve variability. The inner range of 1075 to 31956 again shows the substantial variability in the life estimate indicating a serious instability in the fatigue life computation approach when even small uncertainties exist in assuming a specified spectrum load. Load spectrum and fatigue strength CVs in the range of 7% to 13% are being considered by the helicopter industry.[17] A comparison of the reliabilities of 0.99 and 0.999999 for the respective lifetimes showed 1702 and 448 passes which is a 74% decrease in lifetime. This is a much greater percent decrease than that of the 1% variability case in Figure 8. This assumed variability is probably more realistic than that of 1% which was previously assumed.

Comparison of these figures show uncertainties in safe life fatigue design in terms of changes in design lifetime for a fixed reliability, whereas the results in Tables 1 through 4 show variability in terms of changes in reliability for fixed lifetimes.

Although only a simple case has been considered, the modeling and simulation processes are capable of dealing with more complex safe life fatigue designs. Such designs could include more complex load spectra and additional parameters in the fatigue life model. The value of any high reliability based analyses, whether simple or complex, appears to be in question in view of the very substantial sensitivity of the reliability and lifetime results from this study.

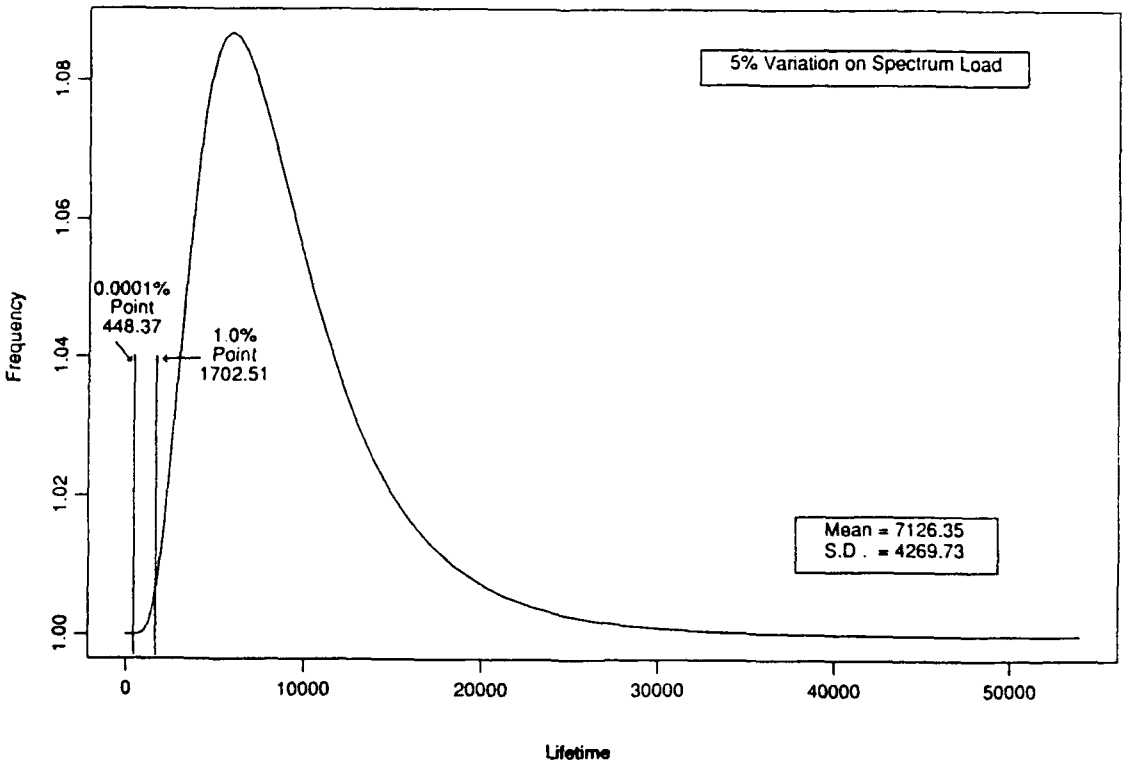

Figure 9. Component fatigue life probability density function and reliability.

CONCLUSIONS

A small amount of variability (uncertainty) in load or strength in the safe life fatigue model can result in a substantial reduction in high reliability values for a specified lifetime of a component. These uncertainties can also result in very unstable lifetime estimates for a given reliability. In contrast, the small variations assumed in the Miner's Rule criterion, and the variability in the SN coupon curve determination, caused a minimal amount of change in the reliability estimates.

A small percent reduction in the strength values in the component SN curve; for example, corrosion effects, can result in a large decrease in the reliability values.

Introducing working curves in the fatigue life computation is only effective when there is a small amount of variability in the SN component curve or when the reduction factor was very large.

In view of the sensitivity of the safe life reliability criterion of 0.999999 to the modest variability considered in this analysis, it appears that the 0.999999 reliability is ineffective as a criterion to ensure safety for a specified service life. **In summary, this report has identified a potential problem associated with obtaining a meaningful quantitative measure of reliability for a fatigue loaded component.**

REFERENCES

1. ARDEN, R. W. *Hypothetical Fatigue Life Problems*. Proceedings of the American Helicopter Society, Midwest Region, Helicopter Fatigue Methodology Specialists' Meeting, March 1980.
2. ARDEN, R. W., and IMMEN, F. H. *U.S. Army Requirements for Fatigue Integrity*. Proceedings of the American Helicopter Society National Technical Specialists' Meeting on Advanced Rotorcraft Structures, Williamsburg, VA, October 1988.
3. AMER, K. B. *A New Philosophy of Structural Reliability, Fail Safe Versus Safe Life*. Journal of the American Helicopter Society, v. 34, no. 1, January 1989.
4. KRASNOWSKI, B. R. *Designing Rotorcraft Dynamics Components to Reliability Requirements*. Presented at the National Fatigue Specialists' Meeting, American Helicopter Society, Scottsdale, AZ, October 1989.
5. SPIGEL, B. S. *Safe Life Design for Rotorcraft*. Journal of the American Helicopter Society, v. 36, no. 1, January 1991.
6. THOMPSON, A. E., and ADAMS, D. O. *A Computational Method for the Determination of Structural Reliability of Helicopter Dynamic Components*. Presented at the American Helicopter Society Annual Forum, Washington DC, May 1990.
7. EVERETT, R. A., BARTLETT, F. D., and ELBER, W. *Probabalistic Fatigue Methodology for Six Nines Reliability*. AVSCOM Technical Report 90-B-009, NASA Technical Memorandum 102757, December 1990.
8. NEAL, D. M., MATHEWS, W. T., and VANGEL, M. G. *Model Sensitivity in Stress-Strength Reliability Computations*. U.S. Army Materials Technology Laboratory, MTL TR 91-3, January 1991.
9. MINER, M. A. *Cumulative Damage in Fatigue*. Journal of Applied Mechanics, v. 12, 1945, p. A150-A164.
10. BURY, K. V. *Statistical Models in Applied Science*. John Wiley & Sons, 1975, p. 598.
11. BERENS, A. P. *Helicopter Fatigue Methodology*. University of Dayton Report, AVSCOM TR-87-D-13A, v. 1, December 1987.
12. WEIBULL, W. *Fatigue Testing and Analysis of Results*. Pergamon Press, New York, NY, 1961.
13. "RNLIN," IMSL Stat/Library: FORTRAN Subroutines for Statistical Analysis, v. 1, ch. 2, April 1987, p. 239-247.
14. EFRON, B. *Bootstrap Methods: Another Look at the Jackknife*. Annals of Statistics, v. 7, 1979, p. 1-26.
15. GUNSALLUS, C. T., HARDERSEN, C. P., and STENNETT, P. G. *Investigation of Fatigue Methodology*. US-AAVSCOM TR 87-D-17, U.S. Army Aviation Applied Technology Directorate, Ft. Eustis, VA, May 1988.
16. NOBACK, R. *State of the Art and Statistical Aspects of Helicopter Fatigue Substantiation Procedures*. Helicopter Fatigue Life Assessment, AGARD CP No. 297, North Atlantic Treaty Organization, March 1981.
17. SCHNEIDER, G., and GUNSALLUS, C. *Continuation of the AHS Round Robin on Fatigue Reliability and Damage Tolerance*. Presented at the American Helicopter Society 47th Annual Forum, Phoenix, AZ, May 1991.

APPENDIX

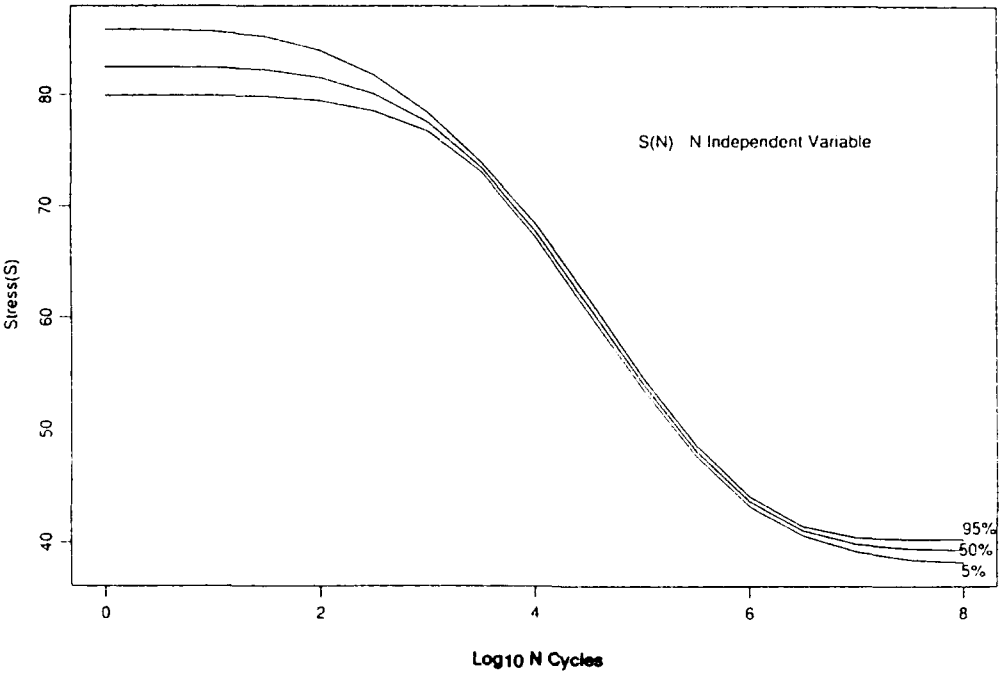

Figure A1. Confidence interval on mean coupon SN curve obtained from fatigue data.

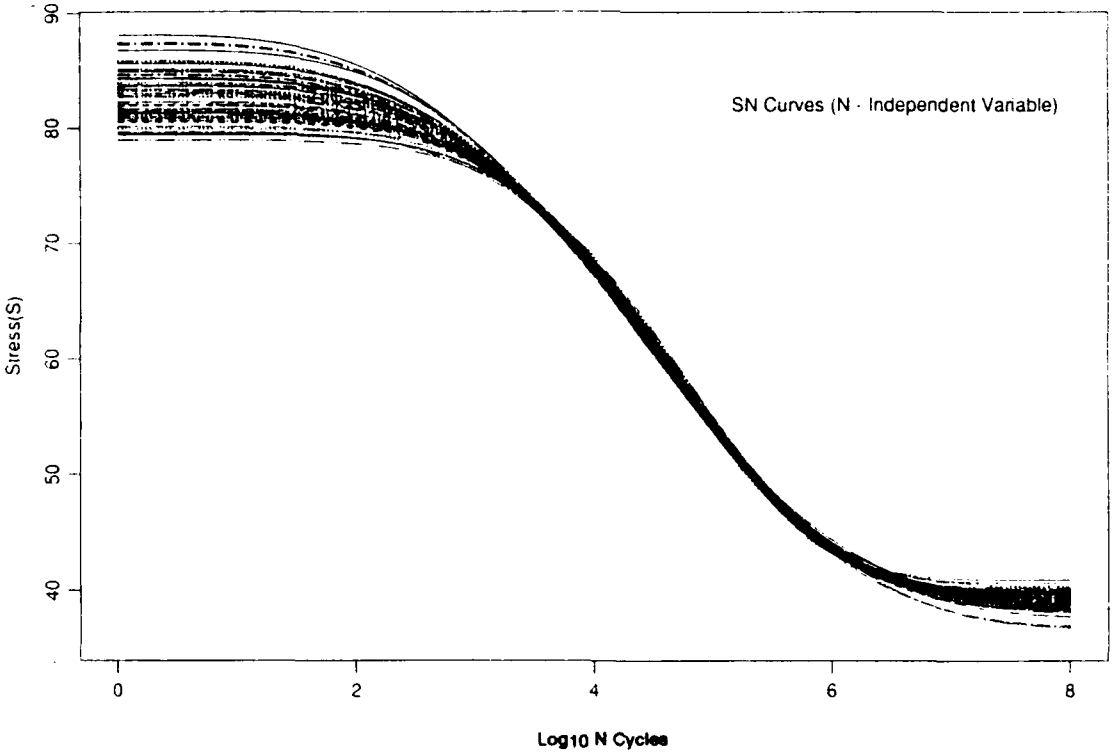

Figure A2. Regression SN curves from Bootstrapping (N-independent variable).

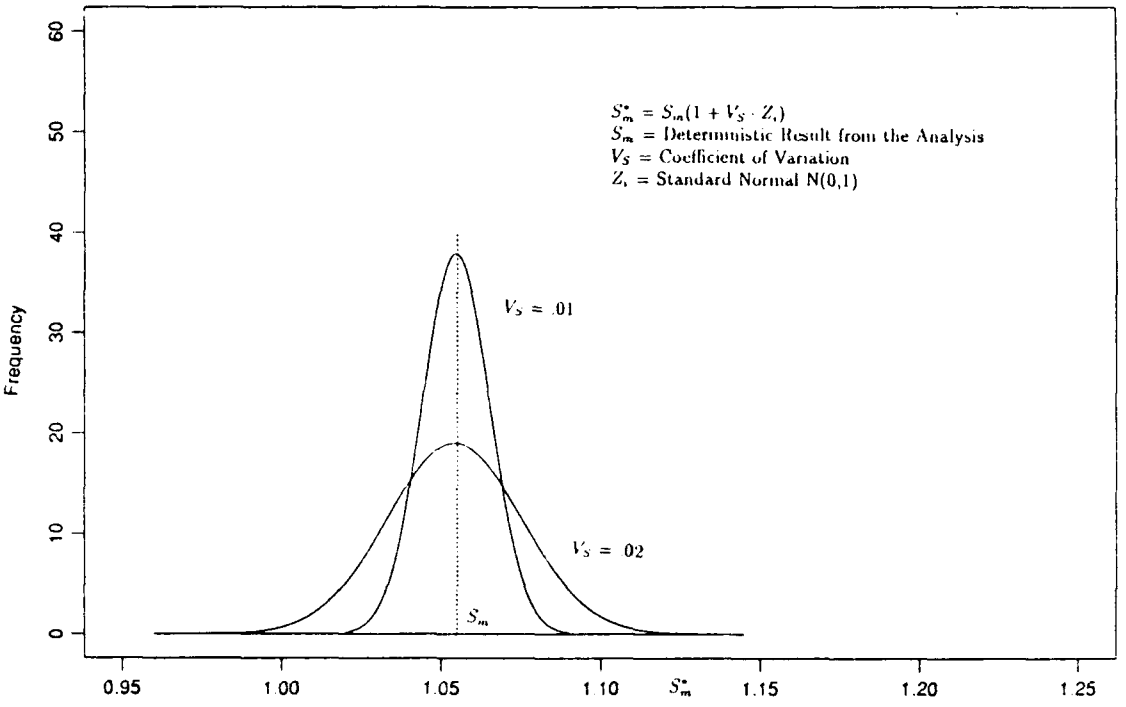

Figure A3. PDF component curve mean value.

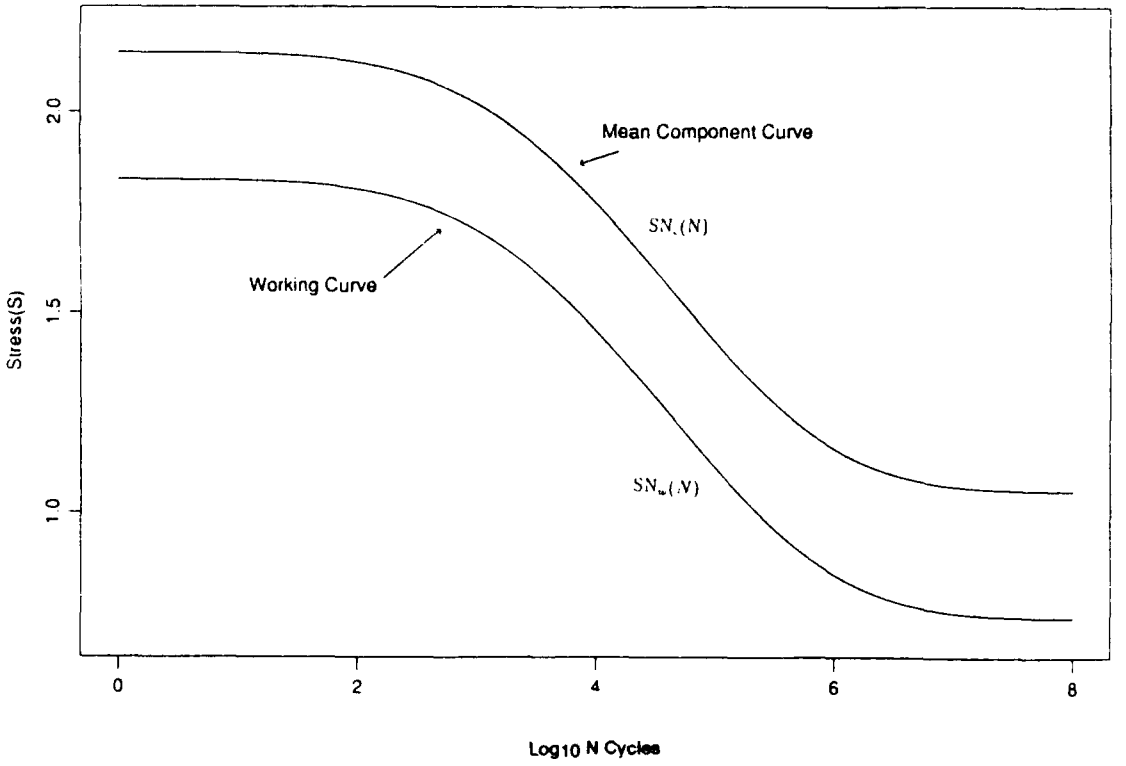

Figure A4. Mean and working component SN curves.

DISTRIBUTION LIST

No. of Copies	To
1	Office of the Under Secretary of Defense for Research and Engineering, The Pentagon, Washington, DC 20301
	Commander, U.S. Army Laboratory Command, 2800 Powder Mill Road, Adelphi, MD 20783-1145
1	ATTN: AMSLC-IM-TL
1	AMSLC-CT
	Commander, Defense Technical Information Center, Cameron Station, Building 5, 5010 Duke Street, Alexandria, VA 22304-6145
2	ATTN: DTIC-FDAC
1	MIAC/CINDAS, Purdue University, 2595 Yeager Road, West Lafayette, IN 47905
	Commander, Army Research Office, P.O. Box 12211, Research Triangle Park, NC 27709-2211
1	ATTN: Information Processing Office
	Commander, U.S. Army Materiel Command, 5001 Eisenhower Avenue, Alexandria, VA 22333
1	ATTN: AMCSCI
	Commander, U.S. Army Materiel Systems Analysis Activity, Aberdeen Proving Ground, MD 21005
1	ATTN: AMXSY-MP, H. Cohen
	Commander, U.S. Army Missile Command, Redstone Scientific Information Center, Redstone Arsenal, AL 35898-5241
1	ATTN: AMSMI-RD-CS-R/Doc
1	AMSMI-RLM
	Commander, U.S. Army Armament, Munitions and Chemical Command, Dover, NJ 07801
1	ATTN: Technical Library
	Commander, U.S. Army Natick Research, Development and Engineering Center, Natick, MA 01760-5010
1	ATTN: Technical Library
	Commander, U.S. Army Satellite Communications Agency, Fort Monmouth, NJ 07703
1	ATTN: Technical Document Center
	Commander, U.S. Army Tank-Automotive Command, Warren, MI 48397-5000
1	ATTN: AMSTA-ZSK
1	AMSTA-TSL, Technical Library
	Commander, White Sands Missile Range, NM 88002
1	ATTN: STEWS-WS-VT
	President, Airborne, Electronics and Special Warfare Board, Fort Bragg, NC 28307
1	ATTN: Library
	Director, U.S. Army Ballistic Research Laboratory, Aberdeen Proving Ground, MD 21005
1	ATTN: SLCBR-TSB-S (STINFO)
	Commander, Dugway Proving Ground, Dugway, UT 84022
1	ATTN: Technical Library, Technical Information Division
	Commander, Harry Diamond Laboratories, 2800 Powder Mill Road, Adelphi, MD 20783
1	ATTN: Technical Information Office
	Director, Benet Weapons Laboratory, LCWSL, USA AMCCOM, Watervliet, NY 12189
1	ATTN: AMSMC-LCB-TL
1	AMSMC-LCB-R
1	AMSMC-LCB-RM
1	AMSMC-LCB-RP
	Commander, U.S. Army Foreign Science and Technology Center, 220 7th Street, N.E., Charlottesville, VA 22901-5396
3	ATTN: AIFRTC, Applied Technologies Branch, Gerald Schlesinger
1	Plastics Technical Evaluation Center, (PLASTEC), ARDEC, Bldg. 355N, Picatinny Arsenal, NJ 07806-5000
	Commander, U.S. Army Aeromedical Research Unit, P.O. Box 577, Fort Rucker, AL 36360
1	ATTN: Technical Library

No. of Copies	To
	Commander, U.S. Army Aviation Systems Command, Aviation Research and Technology Activity, Aviation Applied Technology Directorate, Fort Eustis, VA 23604-5577
1	ATTN: SAVDL-E-MOS
	U.S. Army Aviation Training Library, Fort Rucker, AL 36360
1	ATTN: Building 5906-5907
	Commander, U.S. Army Agency for Aviation Safety, Fort Rucker, AL 36362
1	ATTN: Technical Library
	Commander, USACDC Air Defense Agency, Fort Bliss, TX 79916
1	ATTN: Technical Library
1	Clarke Engineer School Library, 3202 Nebraska Ave. North, Ft. Leonard Wood, MO 65473-5000
	Commander, U.S. Army Engineer Waterways Experiment Station, P. O. Box 631, Vicksburg, MS 39180
1	ATTN: Research Center Library
	Commandant, U.S. Army Quartermaster School, Fort Lee, VA 23801
1	ATTN: Quartermaster School Library
	Naval Research Laboratory, Washington, DC 20375
1	ATTN: Code 5830
1	Dr. G. R. Yoder - Code 6384
	Chief of Naval Research, Arlington, VA 22217
1	ATTN: Code 471
1	Edward J. Morrissey, WRDC/MLTE, Wright-Patterson Air Force, Base, OH 45433-6523
	Commander, U.S. Air Force Wright Research & Development Center, Wright-Patterson Air Force Base, OH 45433-6523
1	ATTN: WRDC/MLLP, M. Forney, Jr.
1	WRDC/MLBC, Mr. Stanley Schulman
	NASA - Marshall Space Flight Center, MSFC, AL 35812
1	ATTN: Mr. Paul Schuerer/EH01
	U.S. Department of Commerce, National Institute of Standards and Technology, Gaithersburg, MD 20899
1	ATTN: Stephen M. Hsu, Chief, Ceramics Division, Institute for Materials Science and Engineering
1	Committee on Marine Structures, Marine Board, National Research Council, 2101 Constitution Ave., N.W., Washington, DC 20418
1	Librarian, Materials Sciences Corporation, 930 Harvest Drive, Suite 300, Blue Bell, PA 19422
1	The Charles Stark Draper Laboratory, 68 Albany Street, Cambridge, MA 02139
	Wyman-Gordon Company, Worcester, MA 01601
1	ATTN: Technical Library
	General Dynamics, Convair Aerospace Division, P.O. Box 748, Fort Worth, TX 76101
1	ATTN: Mfg. Engineering Technical Library
1	Department of the Army, Aerostructures Directorate, MS-266, U.S. Army Aviation R&T Activity - AVSCOM, Langley Research Center, Hampton, VA 23665-5225
1	NASA - Langley Research Center, Hampton, VA 23665-5225
1	U.S. Army Propulsion Directorate, NASA Lewis Research Center, 2100 Brookpark Road, Cleveland, OH 44135-3191
1	NASA - Lewis Research Center, 2100 Brookpark Road, Cleveland, OH 44135-3191
1	Mr. John Adelmann, Sikorsky Aircraft Division, UTC, 6900 Main St., MS S309A, Stratford, CT 06601
1	Mr. Bernard H. Beal, Fairchild Aerospace Fastener Div., 19 Cliftwood Drive, Huntington, NY 11743
1	Dr. Jaclaw Gerrzynski, Boeing Helicopters, P.O. Box 16858, M/S P88-15 Philadelphia, PA 19142
1	Mr. Tom Bitzer, Hexcel, 11711 Dublin Boulevard, Dublin, CA 94568

No. of Copies	To
1	Mr. Gregg Bogucki, McDonnell Douglas Helicopter Co., 5000 E. McDowell Road., MS 531/C235, Mesa, AZ 85205-9797
1	Mr. Patrick M. Brady, Materials Sciences Corporation, 930 Harvest Drive, Suite 300, Blue Bell, PA 19422
1	Dr. Eugene T. Camponeschi, David Taylor Research Center, Code 2802, Annapolis, MD 21402-5067
1	Mr. Frank S. Gruber, General Electric Aircraft Engines, One Neumann Way, MD-H85, Cincinnati, OH 45215-6301
1	Mr. Gary Hansen, Hercules, P.O. Box 98, Magna, UT 84044
1	Dr. L. J. Hart-Smith, Douglas Aircraft Company, Mail Stop 19-98, Long Beach, CA 90846
1	Mr. Philip J. Haselbauer, U.S. Army Aviation Systems Command, AMSAV-EFM, 4300 Goodfellow Blvd., St. Louis, MO 63120-1798
1	Mr. Ray Horton, Boeing, Box 3707, M.S. 3T-CH, Seattle, WA 98124
1	Mr. Steve Jackson, LTV Aerospace, P.O. Box 655907, Dallas, TX 75265-5907
1	Mr. Ted Kruhmin, BP Chemicals (U.S. Polymeric), 700 E. Dyer Road, Santa Ana, CA 92707
1	Mr. A. Hans Magiso, Boeing Helicopters, P.O. Box 16858, MS P32-38, Philadelphia, PA 19142
1	Dr. Crystal H. Newton, Materials Sciences Corporation, 930 Harvest Drive, Suite 300, Blue Bell, PA 19422
1	Mr. Raymond A. Rawlinson, General Electric Aircraft Engines, One Neumann Way, Cincinnati, OH 45215
1	Mrs. Jennifer Rogers, General Dynamics, Fort Worth Div., P.O. Box 748, MZ 6470, Fort Worth, TX 76101
1	Dr. Fritz Scholz, Boeing Computer Services P.O. Box 24346, MS 7L-22, Seattle, WA 98124-0346
1	Mr. E. J. Shahwan, Bell Helicopter Textron, Inc., P.O. Box 482, M/S 4, Fort Worth, TX 76101
1	Mr. Peter Shyprykevich, Grumman Aircraft Systems MS 844-35, Bethpage, NY 11714
1	Mr. Joseph Soderquist, Federal Aviation Admin, AIR-103, 800 Independence Avenue, SW, Washington, DC 20591
1	Mr. Barry Spigel, U.S. Army Aviation Appl Tech Dir., (AVSCOM), ATTN: SAVRT-TY-ATS, Ft. Eustis, VA 23604-5577
1	Mr. Frank Traceski, OSD/DASD (PR), 5203 Leesburg Pike, Suite 1403, Falls Church, VA 22041
1	Mr. Terry Vandiver, U.S. Army Missile Command, ATTN: AMSMI-RD-ST-CM, Redstone Arsenal, AL 35898-5247
1	Mr. Ronald F. Zabora, Boeing Commercial Airplane Group, P.O. Box 3707, MS 9R-61, Seattle, WA 98124
1	Mr. Ted R. Zimmerman, U.S. Army Tank-Automotive Command, ATTN: AMSTA-CR, Warren, MI 48397-5000
1	Mr. Richard Fields, Martin Marrietta, P.O. Box 623007, Mail Stop 1404, Orlando, FL 32862
1	Ms. Cecil Turgeon, Bell Helicopters, Textron, 12800 Rue De L'Avenir, St. Janvier, Quebec JØNILØ
1	Mr. Tom Preece, R+D Ronr Industries, P.O. Box 878, Mail Zone 19T, Chala Vista, CA 92012-0878
2	Director, U.S. Army Materials Technology Laboratory, Watertown, MA 02172-0001 ATTN: SLCMT-TML
4	Authors

U.S. Army Materials Technology Laboratory
Watertown, Massachusetts 02172-0001
A SENSITIVITY ANALYSIS ON COMPONENT RELIABILITY FROM FATIGUE LIFE COMPUTATIONS -
Donald M. Neal, William T. Mathews, Treavor D. Rudalevige, and Mark G. Vangel

Technical Report MTL TR 92-5, February 1992, 23 pp-illus-tables,

AD__________
UNCLASSIFIED
UNLIMITED DISTRIBUTION

Key Words

Reliability
Fatigue life
Flight loads

This paper identifies some uncertainties in determining high component reliability at a specified lifetime from a case study involving the fatigue life of a helicopter component. Reliabilities are computed from results of a simulation process involving an assumed variability (standard deviation) of the load and strength in determining fatigue life. The uncertainties in the high reliability computation are then examined by introducing small changes in the variability for the given load and strength values in the study. Results showed that for a given component lifetime a small increase in variability of load or strength produced large differences in the component reliability estimates. Among the factors involved in computing fatigue lifetimes, the component reliability estimates were found to be most sensitive to variability in loading. Component fatigue life probability density functions were obtained from the simulation process for various levels of variability. The range of life estimates were very large for relatively small variability in load and strength.

U.S. Army Materials Technology Laboratory
Watertown, Massachusetts 02172-0001
A SENSITIVITY ANALYSIS ON COMPONENT RELIABILITY FROM FATIGUE LIFE COMPUTATIONS -
Donald M. Neal, William T. Mathews, Treavor D. Rudalevige, and Mark G. Vangel

Technical Report MTL TR 92-5, February 1992, 23 pp-illus-tables,

AD__________
UNCLASSIFIED
UNLIMITED DISTRIBUTION

Key Words

Reliability
Fatigue life
Fli-'it loads

This paper identifies some uncertainties in determining high component reliability at a specified lifetime from a case study involving the fatigue life of a helicopter component. Reliabilities are computed from results of a simulation process involving an assumed variability (standard deviation) of the load and strength in determining fatigue life. The uncertainties in the high reliability computation are then examined by introducing small changes in the variability for the given load and strength values in the study. Results showed that for a given component lifetime a small increase in variability of load or strength produced large differences in the component reliability estimates. Among the factors involved in computing fatigue lifetimes, the component reliability estimates were found to be most sensitive to variability in loading. Component fatigue life probability density functions were obtained from the simulation process for various levels of variability. The range of life estimates were very large for relatively small variability in load and strength.

U.S. Army Materials Technology Laboratory
Watertown, Massachusetts 02172-0001
A SENSITIVITY ANALYSIS ON COMPONENT RELIABILITY FROM FATIGUE LIFE COMPUTATIONS -
Donald M. Neal, William T. Mathews, Treavor D. Rudalevige, and Mark G. Vangel

Technical Report MTL TR 92-5, February 1992, 23 pp-illus-tables,

AD__________
UNCLASSIFIED
UNLIMITED DISTRIBUTION

Key Words

Reliability
Fatigue life
Flight loads

This paper identifies some uncertainties in determining high component reliability at a specified lifetime from a case study involving the fatigue life of a helicopter component. Reliabilities are computed from results of a simulation process involving an assumed variability (standard deviation) of the load and strength in determining fatigue life. The uncertainties in the high reliability computation are then examined by introducing small changes in the variability for the given load and strength values in the study. Results showed that for a given component lifetime a small increase in variability of load or strength produced large differences in the component reliability estimates. Among the factors involved in computing fatigue lifetimes, the component reliability estimates were found to be most sensitive to variability in loading. Component fatigue life probability density functions were obtained from the simulation process for various levels of variability. The range of life estimates were very large for relatively small variability in load and strength.

U.S. Army Materials Technology Laboratory
Watertown, Massachusetts 02172-0001
A SENSITIVITY ANALYSIS ON COMPONENT RELIABILITY FROM FATIGUE LIFE COMPUTATIONS -
Donald M. Neal, William T. Mathews, Treavor D. Rudalevige, and Mark G. Vangel

Technical Report MTL TR 92-5, February 1992, 23 pp-illus-tables,

AD__________
UNCLASSIFIED
UNLIMITED DISTRIBUTION

Key Words

Reliability
Fatigue life
Flight loads

This paper identifies some uncertainties in determining high component reliability at a specified lifetime from a case study involving the fatigue life of a helicopter component. Reliabilities are computed from results of a simulation process involving an assumed variability (standard deviation) of the load and strength in determining fatigue life. The uncertainties in the high reliability computation are then examined by introducing small changes in the variability for the given load and strength values in the study. Results showed that for a given component lifetime a small increase in variability of load or strength produced large differences in the component reliability estimates. Among the factors involved in computing fatigue lifetimes, the component reliability estimates were found to be most sensitive to variability in loading. Component fatigue life probability density functions were obtained from the simulation process for various levels of variability. The range of life estimates were very large for relatively small variability in load and strength.